

A comparative study of the plastic behaviour of icosahedral and ξ' -Al–Pd–Mn

M. Feuerbacher^{a,*}, H. Klein^a, M. Bartsch^b, U. Messerschmidt^b, K. Urban^a

^a *Institut für Festkörperforschung, Forschungszentrum Jülich GmbH, D-52425 Jülich, Germany*

^b *Max-Planck-Institut für Mikrostrukturphysik, Weinberg 2, D-06120 Halle, Saale, Germany*

Received 3 September 1999; accepted 29 February 2000

Abstract

In the Al–Pd–Mn system, large single crystals of high structural quality can be grown of the icosahedral and the ξ' -phase. The latter is an approximant of the icosahedral phase. Though the structure of ξ' -Al–Pd–Mn is periodic, it possesses a local order which is very close to that of the icosahedral phase. In this paper, we present a comparative study of the plastic behaviour of single crystals of the icosahedral and the ξ' -phase. © 2000 Elsevier Science B.V. All rights reserved.

Keywords: Quasicrystals; Approximants; Plastic deformation; Dislocations

1. Introduction

Quasicrystals are materials showing long-range order but no translational symmetry. Since the well established understanding of crystal plasticity, e.g. the dislocation concept and the concept of dislocation slip are based on the translational symmetry of a crystal lattice, the investigation of quasicrystal plasticity is a priori of great interest. Indeed, experimental deformation studies on quasicrystalline materials have revealed a number of features, which fundamentally differ from those of crystalline alloys. The most remarkable of these salient properties is the absence of work hardening.

It was shown that despite the aperiodic nature of the structure dislocations in quasicrystals, as in crystals, mediate plastic deformation in icosahedral [1] and decagonal [2] quasicrystals. First plastic deformation experiments were performed on poly-quasicrystalline samples of different icosahedral phases [3,22,23]. Subsequent studies were mainly performed on single quasicrystalline Al–Pd–Mn, an icosahedral quasicrystal, which can be grown in the form of large single grains of high structural quality allowing for the determination of the intrinsic deformation properties. These studies include the determination of the thermodynamic activation parameters [4], transmission electron microscopy (TEM) studies of deformed material [5] revealing microstructural deformation parameters, and the performance of in situ straining tests in a high-voltage electron micro-

scope [6]. A model for the description of the plastic properties of icosahedral quasicrystals based on these experimental results, the cluster friction model, was proposed by Feuerbacher et al. [7]. This model was elaborated quantitatively by Messerschmidt et al. [8] on the basis of a Labusch–Schwartz theory. Later studies on single-quasicrystalline samples were performed on icosahedral Zn–Mg–Dy [9], decagonal Al–Ni–Co [2] and Al–Cu–Co [10].

In this paper, we present a comparison of the results of uniaxial plastic deformation experiments on single crystals of the icosahedral and the ξ' -phase in the Al–Pd–Mn system. The ξ' -phase is an approximant of the icosahedral phase. It has an orthorhombic unit cell of space group Pnma with cell parameters $a=23.541$ Å, $b=16.566$ Å and $c=12.339$ Å and, as the icosahedral phase, contains pseudo Mackay clusters as basic structural elements [11]. For this material, a dislocation-free deformation mode showing a deformation process mediated by phason-line defects has been proposed [12]. Nevertheless, dislocations have been observed in this material [13]. A special class of dislocations possessing $[001]$ Burgers vectors and line directions along $[010]$ were found to be decorated by half planes of phason lines inserted into the structure. These defects have been termed metadislocations [13].

2. Experimental procedures

The plastic deformation studies described in this paper were performed on single crystalline and single quasi-

* Corresponding author. Tel.: +49-2461-612409; fax: +49-2461-612409. E-mail address: m.feuerbacher@fz-juelich.de (M. Feuerbacher).

crystalline samples. We have applied the Czochralski and the Bridgman technique for the growth of large single grains of the icosahedral and the ξ' -phase in the Al–Pd–Mn alloy system, respectively. The final compositions of the materials were determined as Al_{70.5}Pd₂₁Mn_{8.5} (icosahedral phase) and Al_{73.9}Pd_{22.2}Mn_{3.9} (ξ' -phase).

Cuboid-shaped compression samples, the long axis along the compression direction, were cut by means of a wire saw. All surfaces were ground and polished in order to prevent cracking due to surface roughness. The faces of the samples of the icosahedral phase were all oriented perpendicular to twofold directions. For the ξ' -phase, the orientation of the samples was chosen such that the compression direction is tilted by 45° with respect to the [100] direction, and the [010] direction is perpendicular to one of the side faces.

Uniaxial plastic deformation experiments were performed in compression under closed-loop-controlled constant-strain-rate conditions. The standard strain rate was chosen as 10⁻⁵ s⁻¹. The strain was measured directly between the compression anvils. All deformations were performed in air. Stress relaxation experiments and strain-rate changes were applied to determine the activation volume V of the deformation process. Temperature change experiments allowed for the evaluation of the activation enthalpy ΔH .

After deformation, the samples were rapidly unloaded and quenched in water within less than 20 s. Specimens for TEM investigation were cut from the deformation samples by wire saw. They were subsequently ground, polished and thinned by Argon ion milling on a liquid nitrogen cooled stage. TEM studies were performed using JEOL 2000EX and 4000FX microscopes operated at 200 kV.

3. Experimental results

3.1. Icosahedral Al–Pd–Mn

Icosahedral Al–Pd–Mn shows brittle behaviour at temperatures below about 75% of the melting temperature at strain rates of 10⁻⁵ s⁻¹. At higher temperatures the material shows extensive ductility.

Fig. 1 shows true stress–true strain curves at a strain rate of 10⁻⁵ s⁻¹ for three temperatures in the ductile regime. After the elastic regime all curves reach an upper yield point. Then a yield drop of about 10–15% of the maximum stress occurs. At higher strains the curves show a steady-state regime of nearly constant flow stress up to about 2–4% followed by a continuous decrease of the flow stress with increasing strain, i.e. a softening behaviour.

The activation volume V of icosahedral Al–Pd–Mn [4] shows values between 1.2 and 0.2 nm³ at 120 and 750 MPa, respectively, and a hyperbolic stress dependence (Fig. 3, solid squares). The stress exponent amounts to about five. The activation enthalpy is generally found to be rather high. Values of about 7 eV [4] linearly increasing with temperature

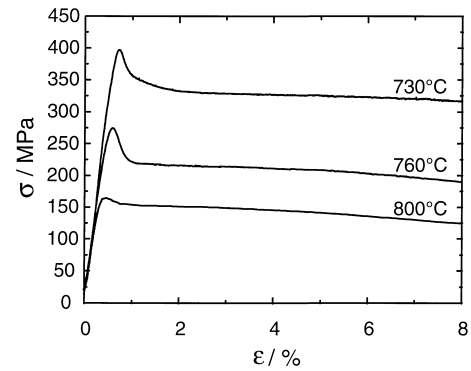


Fig. 1. Stress–strain curves of icosahedral Al–Pd–Mn at a strain rate of 10⁻⁵ s⁻¹ at three different temperatures.

were obtained. Recent studies, taking into account structure changes during stress relaxation, yielded lower values of about 3–6 eV [14]. The work term, i.e. the part of the work which is supplied by the applied stress, amounts to about 0.35 eV.

Microstructural investigations (TEM) of the deformed material revealed detailed information on the microstructural parameters of plastic deformation. The evolution of the dislocation density during plastic deformation has been investigated by bright field imaging under two-beam conditions in TEM [15]. An increase in the dislocation density of up to about two orders of magnitude (7×10^7 cm⁻² in undeformed material, 1.2×10^{10} cm⁻² in material deformed at 730°C) was detected, and at strains higher than about 5%, a subsequent decrease of the dislocation density to about 50% of the maximum dislocation density is observed.

Burgers vectors of dislocations were analysed by means of convergent beam electron diffraction [5,7]. The six-dimensional Burgers vectors \mathbf{B} in quasicrystals possess components in physical space, the phonon part \mathbf{b}_{\parallel} , and in perpendicular space, the phason part \mathbf{b}_{\perp} . The ratio of the moduli of these components defines the strain accommodation parameter ζ , according to $\zeta = b_{\perp}/b_{\parallel}$ [7]. 90% of the Burgers vectors in deformed material were found to be parallel to twofold directions. They have a Burgers vector length in physical space of 0.183 nm corresponding to $\zeta = \tau^5$. Less frequently two-fold Burgers vectors with physical space lengths of $\tau^{-1} \times 0.183$ nm = 0.113 nm, $\tau^{-2} \times 0.183$ nm = 0.070 nm and of $\tau \times 0.183$ nm = 0.296 nm, corresponding to ζ -values of τ^7 , τ^9 , and τ^3 , respectively, are found (Table 1). Thus there exists a spectrum of Burg-

Table 1
Experimentally observed Burgers vector lengths and ζ -values of dislocations icosahedral Al–Pd–Mn

| ζ | b_{\parallel} (nm) | b_{\perp} (nm) |
|----------|----------------------|------------------|
| τ^3 | 0.296 | 1.25 |
| τ^5 | 0.183 | 2.03 |
| τ^7 | 0.113 | 3.28 |
| τ^9 | 0.070 | 5.31 |

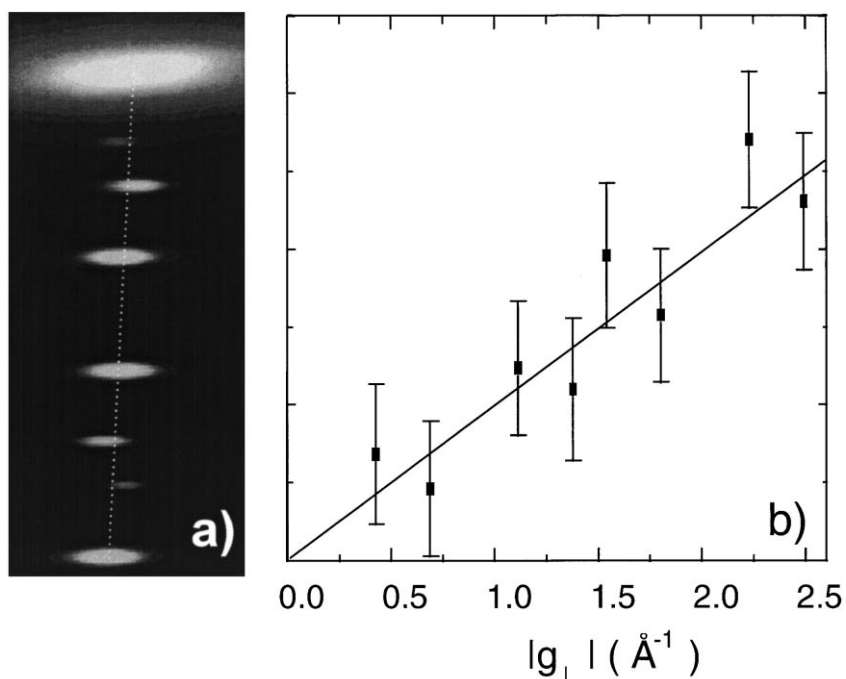


Fig. 2. (a) Systematic row in an electron diffraction pattern showing deviations from the ideal positions of weak spots; (b) dependence of the spot shifts on the magnitude of the perpendicular component of the diffraction vector $|g_{\perp}|$.

ers vector lengths with values according to a τ -sequence descending from τ^3 to τ^9 . Correspondingly, the phason components follow an ascending τ -sequence. The centre of gravity of the distribution curve of experimentally observed ζ -values was observed to depend on plastic strain. With increasing strain the distribution curve shifts towards higher phason components.

Electron diffraction experiments on plastically deformed icosahedral Al–Pd–Mn [16] reveal shifts of low intensity reflections from their ideal positions. Fig. 2 (a) shows a systematic row of a fivefold diffraction pattern as obtained on a sample deformed by 0.25%. The image is shown in perspective view in order to enhance the visibility of the shifts. The dotted line indicates a straight line of ideal reflection positions. The deviations of the spots from this line, being larger for the less intense spots, can be clearly seen. The result of a quantitative determination of the shift vectors is shown in Fig. 2 (b). Plotted as a function of the magnitude of the perpendicular space component g_{\perp} of the corresponding reciprocal lattice vectors a linear dependence on g_{\perp} is observed. The slope of a corresponding linear fit increases with increasing plastic strain. In contrast, represented as a function of the physical space component g_{\parallel} an irregular behaviour occurs. Reference samples, which have not been subjected to deformation do not show detectable shifts of reflections.

These results allow for direct conclusions on the plastic deformation mechanism for icosahedral Al–Pd–Mn. The activation parameters show that the velocity of the dislocations is limited by thermally activated overcoming of obstacles [7]. Due to the lack of translational symmetry moving

dislocations introduce disorder into the material. This is reflected in the electron diffraction studies, showing deviations of low-intensity reflections from their ideal positions. The observed linear dependence on g_{\perp} is a fingerprint behaviour of linear phason strain and can be interpreted quantitatively [16]. This provides direct evidence that linear phason strain is introduced and accumulated in the material during plastic deformation. This is corroborated by the results of Burgers vector determinations showing an increase of the phason component of the Burgers vectors with increasing plastic strain.

3.2. ξ' -Al–Pd–Mn approximant

The present choice of orientation of the deformation samples leads to a maximum shear stress for slip of dislocations with $[001]$ Burgers vectors on (100) planes. Thus, it is expected that the present experiments allow conclusions on plastic deformation of the material due to the slip of metadislocations.

Fig. 4 shows stress–strain curves of ξ' -Al–Pd–Mn samples deformed at a strain rate of 10^{-5} s^{-1} at temperatures between 650 and 750°C. The curves show a number of features, which are due to the tests applied during deformation. The vertical dips are due to stress relaxation tests. One relaxation at 650°C is labelled ‘R’ in the figure. The label ‘TC’ marks a temperature change experiment in the same curve. The label ‘SRC’ marks a strain-rate change applied at 700°C.

At all temperatures, the curves have qualitative features in common. After the elastic regime, yielding occurs in the

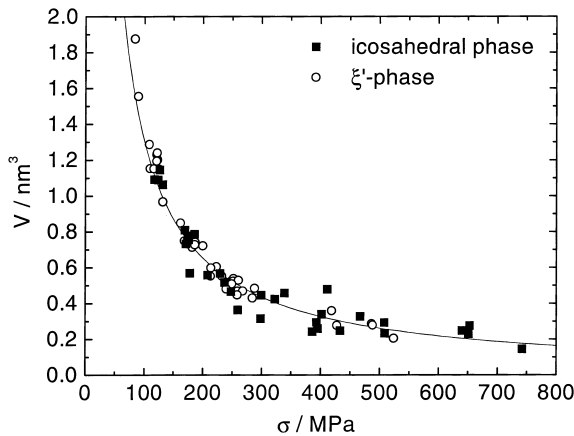


Fig. 3. Activation volume of icosahedral and ξ' -Al–Pd–Mn.

strain range of about 0.4–0.7% followed by a further increase of the flow stress up to a strain of about 2.5–3%. Then, a softening regime occurs at all temperatures, i.e. the stress decreases with increasing strain. The slopes of all hardening and softening stages, considerably decreases with increasing temperature, leading to an almost constant flow stress level at 750°C.

The activation volume ranges from 1.9 nm³ at 70 MPa to 0.2 nm³ at 544 MPa (Fig. 3, solid squares). The stress dependence follows a hyperbolic function. The stress exponent is roughly constant over the stress range of our experiments. Values of about 4.1 are obtained. For the activation enthalpy ΔH we obtain values between 4.2 eV at 655°C and 5.8 eV at 755°C. The work term amounts to 0.4 eV.

Microstructural investigations (TEM) were performed on the material deformed at 700°C by about 0.8% behind the yield point. Thin foil specimens with a foil normal parallel to the [0 1 0] direction were cut from the deformation sample. Bright field imaging under two-beam shows a high density of point-like contrast, due to dislocations with a line direction parallel to [0 1 0] and a Burgers vector parallel to [0 0 1], which are seen in end-on orientation. Their density amounts to about $1.0 \times 10^9 \text{ cm}^{-2}$. The slip plane of these dislocations is the (1 0 0) plane. A second set of dislocations with a line direction perpendicular to the [1 0 2] direction is present at a density of about $4.5 \times 10^7 \text{ cm}^{-2}$, i.e. about two orders of magnitude smaller than the (1 0 0)[0 0 1] slip system.

High resolution imaging of the dislocations with line direction along [0 1 0] shows that these dislocations are metadislocations, i.e. we find phason planes connected to that region of the specimen where we find the dislocations under two-beam conditions. A number of different types of metadislocation could be identified. We found metadislocations with 4, 6, 10 and 16 inserted phason half planes with Burgers vector direction along [0 0 1] [17]. By performing Burgers circuit analyses in the high-resolution images we could identify the lengths of the Burgers vectors of these dislocations b as 0.296, 0.183, 0.113 and 0.070 nm, respectively. (Table 2).

Table 2

Properties of experimentally observed metadislocations in deformed ξ' -Al–Pd–Mn

| b (nm) | Number of half planes |
|----------|-----------------------|
| 0.296 | 4 |
| 0.183 | 6 |
| 0.113 | 10 |
| 0.070 | 16 |

Dislocations with Burgers vectors along other directions have also been found. These are discussed in [18]. Additionally, we observed a high density of phason lines. However, from the present experiments we cannot conclude, how these contribute to the plastic deformation process [16,19].

Direct conclusions on the plastic deformation mechanism can be drawn from these results. The plastic deformation of ξ' -Al–Pd–Mn in the present deformation geometry takes place under participation of dislocation motion, primarily by activation of the (1 0 0)[0 0 1] slip system. The deformation process is thermally activated.

4. Discussion

Icosahedral and ξ' -Al–Pd–Mn are phases, which are close in composition and local order. Structure studies of these materials [11,20] revealed that both possess Mackay-type clusters as basic structural elements. However, ξ' -Al–Pd–Mn is a crystalline approximant and therefore does not have translational symmetry. It is therefore of basic interest to compare the properties of these phases.

The most prominent feature of the macroscopic plasticity of icosahedral Al–Pd–Mn is the lack of work hardening. Hardening stages, i.e. stages of the stress–strain curve with a positive slope in the high-strain region have generally been observed for the case of crystalline alloys. Stress–strain curves showing no hardening as those in Fig. 1 are typical for quasicrystals, and have also been observed e.g. for Zn–Mg–Dy [9] and Al–Ni–Co [2] single quasicrystals.

The origin of the work softening behaviour of icosahedral Al–Pd–Mn was, qualitatively described by the cluster–friction model [7], which assumes the elementary Mackay-type clusters to act as rate-controlling obstacles for dislocation motion. The ordered structure of the original quasicrystal is destroyed locally by the introduction of matching-rule violations, which, on the average, leads to a decrease of the density of obstacles in the course of plastic deformation. Since by this process those elements of the structure, which limit the dislocation velocity are decreased in density, the structure is weakened in the sense that dislocation motion becomes easier.

The stress–strain curves of the ξ' -phase also show no work hardening stages at high strains (Fig. 4). At low temperatures, we find pronounced softening behaviour, i.e. the flow stress is substantially decreasing with increasing strain. With

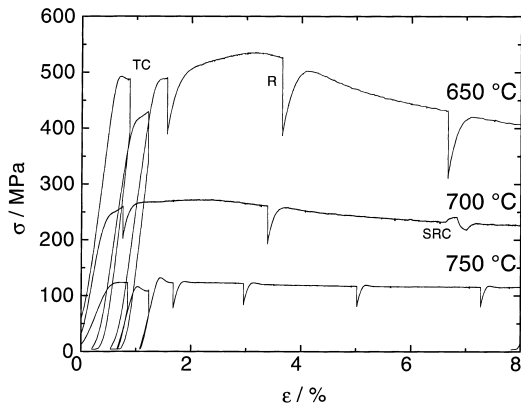


Fig. 4. Stress–strain curves of ξ' -Al–Pd–Mn at a strain rate of 10^{-5} s^{-1} at three different temperatures.

increasing temperatures the slope is getting smaller, leading to an almost constant flow-stress level over the complete high-strain range at 750°C . Thus, with respect to the most prominent feature of quasicrystal deformation, the lack of work hardening, the ξ' -approximant phase shows the same characteristics despite of its translational invariance.

However, we find a number of substantial differences in the stress–strain characteristics of the two phases.

- For ξ' -Al–Pd–Mn, we do not find a distinct upper yield stress or yield drop.
- The slope of the stress–strain curve in the plastic regime strongly depends on the deformation temperature.
- A hardening stage occurs in the lower strain range starting after the elastic regime up to about 2–3.3%. The slope of this hardening stage also depends on the deformation temperature.

For a comparison of the flow stress of the two materials, we refer to the homologous temperature T_H using values for the melting temperature of 870°C for the icosahedral and 845°C for the ξ' -phase. Fig. 5 shows the flow stress of the two materials as a function of T_H . At low temperatures, the

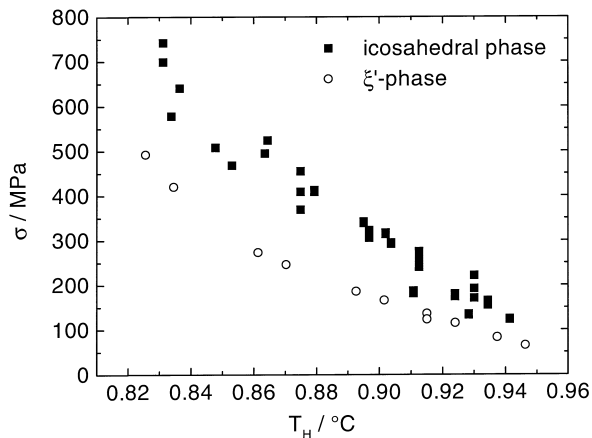


Fig. 5. Comparison of the flow stresses. Solid squares: upper yield stress of the icosahedral phase, open circles: flow stress at the yield point of ξ' -Al–Pd–Mn.

flow stress of ξ' -Al–Pd–Mn is lower by about 200 MPa. At more elevated temperatures the flow stresses become about equal. The temperature dependence of the flow stress is about 3.1 and 4.3 MPa/K for ξ' - and icosahedral Al–Pd–Mn, respectively. This indicates that the activation enthalpy of ξ' -Al–Pd–Mn should be smaller than that of the icosahedral phase, which was indeed observed.

Fig. 3 shows a comparison of the activation volumes of icosahedral Al–Pd–Mn and of ξ' -Al–Pd–Mn. The activation volume, V is characteristic of the activation process in the deformation mechanism. It is influenced by the size and distances of the rate controlling obstacles determining dislocation velocity. As shown in Fig. 3, we find a perfect coincidence of V and its stress dependence for the phases. Thus, we can conclude that the rate controlling mechanisms of icosahedral and ξ' -Al–Pd–Mn are closely related.

Other indications for a close relationship between the plasticity of icosahedral and ξ' -Al–Pd–Mn are provided by the microstructural investigations. The most frequently observed Burgers vector in icosahedral Al–Pd–Mn is parallel to a twofold direction and has a physical-space length of 0.183 nm. In ξ' -Al–Pd–Mn dislocations with twofold $[001]$ Burgers vectors having the same length of 0.183 nm were also detected frequently [13]. This Burgers vector length is an irrational fraction of the lattice parameter $c=12.339 \text{ \AA}$ along the $[001]$ direction. Thus, these dislocations have to be regarded as partials. For structures possessing such large lattice parameters as the ξ' -structure the creation of partials rather than perfect dislocations is unavoidable for energetical reasons. The elastic energy of a dislocation is proportional to the square of the Burgers vector length. Thus, perfect dislocations, i.e. dislocations with a Burgers vector length equal to a lattice constant would be energetically highly unfavourable. The motion of a partial, however, gives rise to the introduction of a stacking fault.

For the case of ξ' -Al–Pd–Mn, the six phason half planes connected to this dislocation provide a means to accommodate the partial dislocation to the surrounding structure. The dislocation with its connected phason half planes as a whole is therefore able to move through the structure without introducing a stacking fault. Thus, by virtue of the metadislocations, on the one hand, the energetically unfavourable high elastic strain fields of a perfect dislocation in the large-unit-cell structure, and on the other hand the creation of stacking faults by motion of partials are avoided. In crystals, of course, partial dislocations exist, and their motion does create stacking faults. However, the creation of permanent stacking faults in the lattice can be avoided by subsequent motion of $n=a/b$ partials, where a is the lattice constant and b is their burgers vector length. For example, in FCC lattices the subsequent motion of two (energetically favourable) $a/2 [110]$ partials only leads to a stacking fault of limited extension between the partials. Since, in ξ' -Al–Pd–Mn the Burgers vector length is an irrational fraction of the lattice constant, such a mechanism of

erasing a previously created stacking fault by a finite number of subsequent partials does not work.

Due to the aperiodic structure of icosahedral Al–Pd–Mn, a dislocation with any physical-space Burgers vector length corresponds to a partial. It has been shown [21] that the phason component of the strain field, which is associated to the phason component of the burgers vector, is necessary to accommodate the dislocation to the structure.

The τ -sequence of values of physical space lengths of Burgers vectors in icosahedral Al–Pd–Mn (Table 1) have without exception also been observed for the dislocations in the ξ' -phase (Table 2). The reverse sequence of the length of the phason parts also possesses its counterpart for the case of ξ' -Al–Pd–Mn. Here the number of inserted phason half planes follow a Fibonacci sequence. We find values of 4, 6, 10, and 16 corresponding to twice the values of the consecutive Fibonacci numbers 2, 3, 5, and 8.

5. Conclusions

Icosahedral and ξ' -Al–Pd–Mn show a number of common features in their macroscopic and microscopic plastic deformation properties. These allow us to conclude that the plastic deformation mechanisms of these materials, though belonging to different classes of solids, are closely related. General conclusions on the role of local order and translational symmetry on the plastic deformation properties can not be drawn at present.

References

- [1] M. Wollgarten, M. Beyss, K. Urban, H. Liebertz, U. Köster, Phys. Rev. Lett. 71 (1993) 549.
- [2] M. Feuerbacher, M. Bartsch, B. Grushko, U. Messerschmidt, K. Urban, Phil. Mag. Lett. 76 (1997) 369.
- [3] S. Kang, J.M. Dubois, Phil. Mag. A 66 (1992) 151.
- [4] M. Feuerbacher, B. Baufeld, R. Rosenfeld, M. Wollgarten, M. Bartsch, U. Messerschmidt, K. Urban, Phil. Mag. Lett. 71 (1995) 91.
- [5] R. Rosenfeld, M. Feuerbacher, B. Baufeld, M. Bartsch, U. Messerschmidt, M. Wollgarten, G. Hanke, M. Beyss, K. Urban, Phil. Mag. Lett. 72 (1995) 375.
- [6] M. Wollgarten, M. Bartsch, U. Messerschmidt, M. Feuerbacher, R. Rosenfeld, M. Beyss, K. Urban, Phil. Mag. Lett. 71 (1995) 99.
- [7] M. Feuerbacher, C. Metzmacher, M. Wollgarten, B. Baufeld, M. Bartsch, U. Messerschmidt, K. Urban, Mater. Sci. Eng. A 233 (1997) 103.
- [8] U. Messerschmidt, M. Bartsch, B. Geyer, M. Feuerbacher, K. Urban, Phil. Mag. A, 2000, in press.
- [9] M. Heggen, M. Feuerbacher, P. Schall, P.C. Canfield, I.R. Fisher, K. Urban, in press.
- [10] K. Edagawa, Y. Arai, T. Hashimoto, S. Takeuchi, Mater. Trans. JIM 38 (1998) 863.
- [11] M. Boudard, H. Klein, M. DeBoissieu, M. Audier, H. Vincent, Phil. Mag. A 74 (1996) 939.
- [12] H. Klein, M. Audier, M. Boudard, M. de Boissieu, L. Beraha, M. Duneau, Phil. Mag. A 73 (1996) 309.
- [13] H. Klein, M. Feuerbacher, P. Schall, K. Urban, Phys. Rev. Lett. 82 (1999) 3468.
- [14] B. Geyer, M. Bartsch, M. Feuerbacher, K. Urban, U. Messerschmidt, Phil. Mag. A, 2000, in press.
- [15] P. Schall, M. Feuerbacher, U. Messerschmidt, M. Bartsch, K. Urban, Phil. Mag. Lett., 2000, in press.
- [16] V. Franz, M. Feuerbacher, M. Wollgarten, K. Urban, Phil. Mag. Lett. 79 (1999) 333.
- [17] H. Klein, M. Feuerbacher, K. Urban, in press.
- [18] H. Klein, M. Feuerbacher, K. Urban, these proceedings.
- [19] H. Klein, M. Feuerbacher, P. Schall, K. Urban, Phil. Mag. Lett., 2000, in press.
- [20] M. Boudard, M. DeBoissieu, C. Janot, G. Heger, C. Beeli, H.-U. Nissen, H. Vincent, R. Ibberson, M. Audier, J.M. Dubois, J. Phys. Cond. Mater. 4 (50) (1992) 10149.
- [21] W. Yang, M. Feuerbacher, N. Tamura, D. Ding, R. Wang, K. Urban, Phil. Mag. A 77 (1998) 1481.
- [22] L. Bresson, D. Gratias, J. Non Cryst. Sol. 153/154 (1993) 468.
- [23] S. Takeuchi, H. Iwanaga, T. Shibuya, Jpn. J. Appl. Phys. 30 (1991) 561.